Solar Energy Materials & Solar Cells 245 (2022) 111854

Contents lists available at ScienceDirect

Solar Energy Materials and Solar Cells

journal homepage: www.elsevier.com/locate/solmat

Sub-ambient daytime radiative cooling based on continuous sunlight blocking

Bin Zhao [a], Kegui Lu [a], Mingke Hu [b], Ke Wang [c], Datong Gao [a], Ken Chen [a], Qingdong Xuan [d], Gang Pei [a,*]

[a] Department of Thermal Science and Energy Engineering, University of Science and Technology of China, Hefei, 230027, China
[b] Department of Architecture and Built Environment, University of Nottingham, University Park, Nottingham, NG7 2RD, UK
[c] School of Electronic Science and Engineering, Nanjing University, Jiangsu, 210046, China
[d] School of Automotive and Transportation Engineering, Hefei University of Technology, Hefei, 230009, China

ARTICLE INFO

Keywords:
Radiative cooling
Passive cooling
Thermal radiation
Atmospheric window

ABSTRACT

Parasitic solar heating of the radiative cooler remarkably counteracts the cooling effect generated by radiative cooling. Many previous works have contributed to improving the solar reflectivity of the cooler to reduce its solar absorption, including using highly reflective film or optimized scattering effect. Herein, an easy and passive sunlight blocking strategy based on geometrical optics is applied to reduce the solar heating power of the cooler by using a ring-like shield to prevent the propagation of direct sunlight, corresponding to decoupling the cooler from solar beam irradiance. A black paint-coated cooler with strong solar absorption of over 0.9 and a porous polytetrafluoroethylene (P-PTFE) cooler with a high solar reflection of over 0.9 are fabricated to demonstrate the feasibility of the sunlight blocking strategy. Results show that radiative cooling to 3.5°C and 6.5°C below ambient temperature under average solar irradiance of 500 W m^{-2} is achieved by the black paint and P-PTFE, revealing that the proposed sunlight blocking strategy contributes to efficient sub-ambient daytime radiative cooling. Theoretical analysis not only proves the effectiveness of the sunlight blocking strategy but also reveals that cooler with selective emission within the atmospheric window is more sensitive to sunlight, as well as capturing the radiative cooling performance under different conditions.

1. Introduction

Cooling technologies are essential for human beings, not only in our ordinary life and the industry but also in the scientific research area. Focusing on cooling with clean methods, passive radiative cooling is a promising technique and has drawn remarkable attention, which can achieve a sub-ambient cooling phenomenon by rejecting thermal energy into the cold universe (~3K) [1–6], mainly relying on the transparency of the atmosphere within the 8-13 μm. Radiative cooling is a natural phenomenon and can be widely observed. For example, the frost and dew water is formed on the top sky-faced surface of the leaf even when the freezing and dew point temperatures are not reached for ambient air. This is because the sky-faced leaf radiates heat to outer space and then gets a local temperature reduction, thus reaching the freezing and dew point temperatures in the local environment [7]. Radiative cooling was previously studied at night for cooling, such as space cooling for buildings [8–11] and nighttime power generation [12–14]. Recently, sub-ambient radiative cooling is well demonstrated based on advanced optical materials [4,5,15,16], which arouse much interest in the fields of renewable energy and optical materials. Compared with common refrigeration techniques, such as vapor compression and absorption refrigeration, radiative cooling can operate passively without any external energy input and this feature makes it to be one of the promising clean cooling methods.

According to the heat transfer analysis, the radiative heat transfer mode dominates the daytime radiative cooling process, which mainly relates to solar radiation and atmospheric radiation. The absorbed solar power of the radiative cooler is in direct proportion to its solar absorptivity and incident solar power. Many efforts have been previously paid to reduce the solar absorptivity of the cooler by optimizing the materials design, such as using a highly reflective cooler and photon-scattered windshield. Generally, radiative coolers are required to highly reflect sunlight and simultaneously exhibit strong thermal emission within the atmospheric window. Raman et al. [17] designed and

* Corresponding author.
E-mail address: peigang@ustc.edu.cn (G. Pei).

https://doi.org/10.1016/j.solmat.2022.111854
Received 17 April 2022; Received in revised form 29 May 2022; Accepted 15 June 2022
Available online 21 June 2022

fabricated a multilayered radiative cooler that can reflect 97% solar irradiance and emit strongly within the atmospheric window, and this cooler can be passive cooled to nearly 5°C below ambient air, experimentally achieving the sub-ambient radiative cooling under sunshine for the first time. Zhai et al. [18] combined a reflective silver film and a particle-embedded polymer matrix to fabricate a scalable-manufactured metamaterial for efficient sub-ambient radiative cooling with a maximum cooling power of over 90 W m^{-2}. Apart from using the solar reflective film, optimized scattering effects have also been developed to reflect sunlight for the radiative cooler. Mandal et al. [19] designed hierarchically porous polymer coatings using the phase-inversion-based method. The fabricated coating has a strong hemispherical solar reflection of 0.96 and high thermal emissivity of 0.97, and a sub-ambient temperature drop of 6°C is experimentally obtained. Similarly, various radiative coolers with high solar reflection and strong thermal emission have been developed, including photonic structures [20–23], porous materials [24–27], and nanoparticle-based paints [28–33].

Applying a solar-reflective infrared-transparent windshield to the top of the radiative cooler is also a feasible method to reduce the solar absorption of the cooler. Torgerson et al. [34] developed a porous polyethylene filter to reflect sunlight and transmit long-wave thermal radiation. The high solar reflection of the porous filter is contributed by the optimized scattering effect. Zhang et al. [35] proposed an optical-reflective infrared-transparent windshield for efficient sub-ambient radiative cooling during daytime. Moreover, mechanical properties [36] and thermal conductivity properties [37] are also integrated with the optical design of the windshield. The core of the above method is to design and optimize the structure of the material for spectrum management. However, tailoring selective spectrum for radiative cooler and windshield both in the solar band and atmospheric window is difficult. Coolers have different requirements in the solar band and atmospheric window, so the parameter determination of the patterned structures needs refined optical simulations and optimizations, such as using the needle method to design multilayer film [17], applying coupled machine learning and electromagnetic calculation to optimize the patterned structures [38]. Moreover, complicated and strict processing methods/equipment, such as etching for 2-dimensional structures [22,39] and multistage deposition for multilayer films [17], are required during the sample fabrication, which is not friendly for real-world applications.

Fortunately, suppressing the solar irradiance received by the cooler on the basis of geometrical optics methods is also a possible solution to reduce the solar absorption of the cooler. Chen et al. [40] used a planar reflective plate to block direct sunlight and a curved surface to block diffuse sunlight. Combined with a vacuum environment, a solar absorptive cooler is also cooled by 40°C below ambient temperature under the sunshine. Our group also proposed a new strategy to block the sunlight by changing the relative position between the radiative coolers and the sun to reduce the direct sunlight to the cooler [41]. Experiment demonstration shows that the commercial cooler with solar absorptivity of 0.66 can also be cooled by 3.2°C on average below the ambient air when the cooler is placed back to the sun with a tilt angle of about 30°C, providing a feasible avenue for common materials to potentially achieve sub-ambient radiative cooling under sunshine. To balance the effect of tilt angles on sunlight blocking and net thermal emission, a small tilt angle of 15°C was selected for sub-ambient radiative cooling and applied in a kW-scale radiative cooling system [42,43]. Moreover, the effect of different tilt angles on radiative cooling performance was also experimentally investigated [44]. However, the sunlight blocking effect of the above methods will be weakened under some conditions, especially when the sun's zenith angle is close to zero. To solve this issue, Bhatia et al. [45] propose a directional sub-ambient radiative cooling strategy by using a mobile solar shield to block the sunlight. Experimental results show a temperature of 6°C below ambient temperature and maximum cooling power of 45 W m^{-2} is achieved around noontime. However, a solar tracking system is required to dynamic control the position of the mobile shield to maintain that the cooler is always covered by the shadow of the shield regardless of the sun's position. Then, the same team further propose possible sunlight blockling methods, including a non-solar-tracking solution, to reduce the effect of direct sunlight, but frequently position operation is also required and experimental demonstrations are also required.

In this work, a passive sunlight blocking strategy without a solar tracking system is proposed to prevent the propagation of direct solar radiation for sub-ambient radiative cooling under sunlight. A shade plate is applied to block direct sunlight for radiative cooler over the entire day without frequent operation for position adjustment. A commercial black paint-coated cooler and a porous polytetrafluoroethylene (P-PTFE) cooler are fabricated for experimental testing to demonstrate the feasibility of the proposed strategy. Moreover, a mathematical model is developed to capture the radiative cooling performance under the strategy of direct sunlight blocking.

2. Experimental demonstration

2.1. Passive sunlight blocking strategy

The position of the sun changes with time regularly, so a shield that can block the sunlight over the whole day for radiative cooler is required for sub-ambient radiative cooling. A ring-like shield (Fig. 1a) rather than a piece of small planar shield is implemented between the sun and the radiative cooler to block the direct sunlight during the day. During the movement of the sun, a series of shadows are generated behind the ring-like shield. If the radiative cooler is fixed within the overlapped region of the shadows, direct sunlight will be successfully blocked. As shown in Fig. 1b, the view factor of the cooler to the sky is only slightly reduced after using the shield, which keeps the cooler to access the clear sky as much as possible and this is a good feature for radiative cooling when a sunlight shelter is applied. Notably, the declination angle of the sun changes for different dates (e.g., summer and winter), so the shield can change the relative position to the cooler according to the different dates for direct sunlight blocking. To further reduce the effect of the diffuse light on the sub-ambient radiative cooling performance, various existing methods, such as using reflective walls [40], can also be applied.

2.2. Material preparation

Two radiative coolers are used for experimental demonstration in this study. One is a black paint-coated cooler and the other is a porous polytetrafluoroethylene (P-PTFE) cooler. The black paint cooler is fabricated by spraying black paint on a thin copper substrate. To ensure that the substrate is fully covered by the black paint and the uniform of the paint, multiple spraying-drying operations are conducted. The natural drying process is conducted during the fabrication. The P-PTFE is fabricated by extruding porous PFTE (Smart Membrane, Xiamen) and aluminum foil together [46].

The spectral reflectivity of the black paint cooler and P-PTFE is characterized and shown in Fig. 2 to investigate their radiative properties, including solar reflection and thermal emissivity. The black paint cooler has a low solar reflection that corresponds to strong solar absorption (over 0.9), while the P-PTFE exhibits a high reflectivity (over 0.9) for sunlight. In the mid-infrared band, both the black paint cooler and P-PTFE show strong thermal emissions within the atmospheric window, respectively. The spectral reflectivity of two coolers within the solar band is measured using a UV–Vis–NIR spectrophotometer (SolidSpec-3700, Shimadzu), and a Fourier Transform Infrared Spectrometer (Nicolet iS10 Thermo Scientific) coupled with a Mid-IR integrating sphere (Mid-IR IntegratIR, Pike Technologies) is applied for measurement in the mid-infrared band. The emissivity of the cooler is then determined based on the energy balance and Kirchhoff's law. During measurement, barium sulfate and gold film are used as the standard reference for testing.

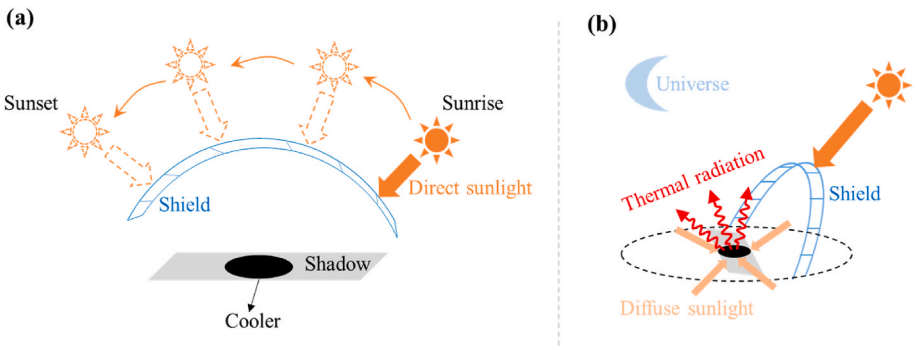

Fig. 1. The schematic of the passive sunlight blocking method.

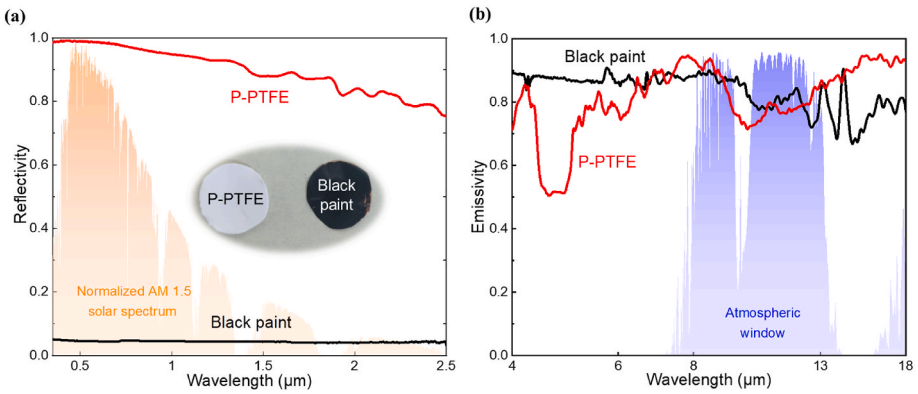

Fig. 2. Spectral properties of the black paint cooler and P-PTFE. (a) Measured solar reflectivity of two coolers with normalized AM 1.5 solar spectrum and optical images of the cooler presented as references. (b) Measured thermal emissivity of two coolers with the transmittance of the atmospheric window plotted as a reference.

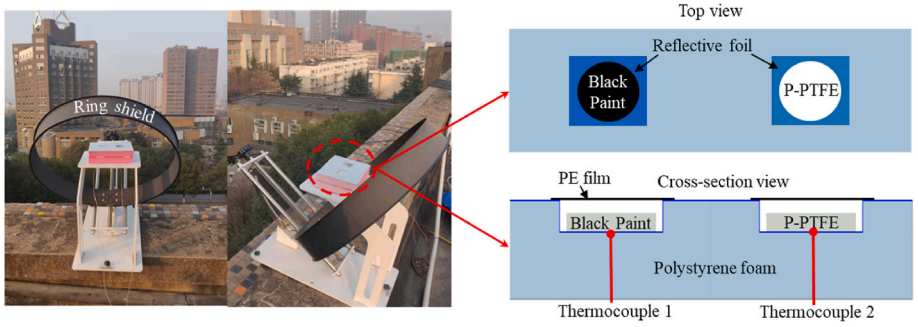

Fig. 3. Photos of the experimental apparatus with a top view and cross-section view of the radiative cooling device given as reference.

2.3. Experimental setup

Outdoor experimental testing (Fig. 3) is conducted to demonstrate the radiative cooling performance under the proposed strategy. The sunlight blocking device (Jinzhou Sunshine Technology Co.Ltd) consists of a black ring shield with a diameter of 40 cm and a width of 6.5 cm and a position control system that contains a screw rod, a scaleplate, and bolts. The metal framework is used as the support. The black paint cooler and P-PTFE are fixed in an air chamber surrounded by polystyrene foam to reduce the heat transfer between the cooler and ambient air. Reflective film is covered on the surface that is exposed to the sun and sky directly. Thin polyethylene (PE) film is placed on the top of the air chamber to decouple the cooler from ambient air, thus improving the sub-ambient radiative cooling performance.

The experimental setup is established on the rooftop of the second building of Mechanics in the University of Science and Technology of China at Hefei, China (32°N, 117°E). Thermocouples are attached to the backside of the black paint and P-PTFE to monitor the real-time temperature. A pyranometer (TBQ-2, Jinzhou Sunshine Technology Co., Ltd) is installed horizontally to measure the total solar irradiance and a pyrgeometer (TBL-1, Jinzhou Sunshine Technology Co., Ltd) is applied to record the downwelling long-wave atmospheric radiation. The wind speed is measured by a wind speed sensor (HSTL-FS01), and ambient temperature and relative humidity are measured using a portable weather station (HSTL-BYXWS). A data logger (LR8450, HIOKI) is used to record all the above data.

2.4. Experimental results

The outdoor experiment was carried out on December 20, 2021, at Hefei, China. The temperature of the black paint cooler and P-PTFE under sunshine is presented in Fig. 4a, with solar irradiance and ambient temperature plotted as references. During testing, the average relative humidity and wind speed are approximately 35% and 0.9 m s^{-1},

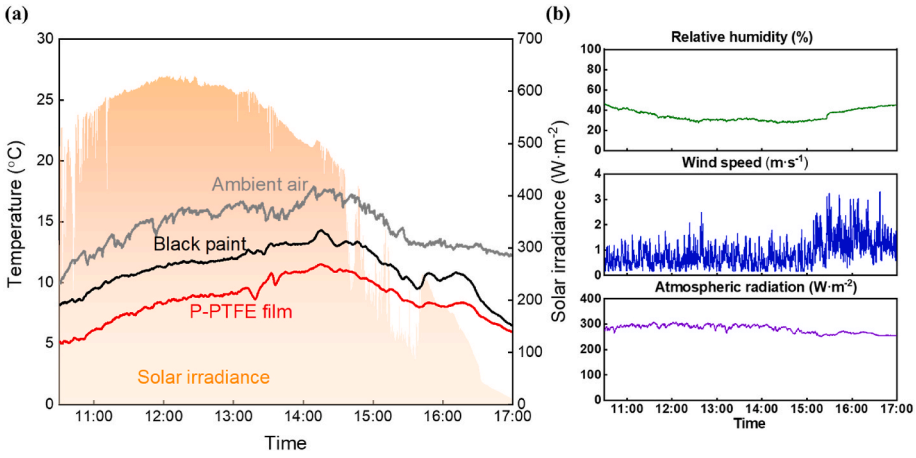

Fig. 4. (a) Measured temperature of the black paint cooler and P-PTFE during the daytime, with solar irradiance and ambient temperature plotted as references. (b) Measured relative humidity, wind speed, and long-wave atmospheric radiation.

respectively. Besides, the average atmospheric long-wave radiation is about 281 W m^{-2}. It is evidenced that the temperature of the cooler is lower than ambient temperature for the entire testing period, though black paint that has strong solar absorption, which shows sub-ambient radiative cooling is achieved, indicating the effectiveness of the proposed passive sunlight blocking strategy for sub-ambient radiative cooling. From 11:00 to 14:00, the average solar irradiance is over 500 W m^{-2}, and the temperature of the black paint cooler and P-PTFE are 11.7°C and 8.7°C, respectively, 3.5°C and 6.5°C lower than ambient temperature. Compared with the black paint cooler, P-PTFE has a high solar reflection that maximally prevents the intrinsic solar heating of the cooler, then further contributing to sub-ambient radiative cooling.

The temperature of the cooler under nighttime was also monitored and presented in Fig. 5. The temperature of the black paint cooler and P-PTFE during the testing period is nearly consistent and this is because the thermal emissivity property of the cooler dominates the heat transfer process under darkness and the thermal emissivity of the two coolers are similar. From 17:30 to 20:30, the temperature of the black paint cooler and P-PTFE are 6.1°C and 6.1°C lower than ambient temperature, demonstrating the temperature consistency. Notably, the sky condition becomes worse within 18:00 to 19:30 due to the cloud cover, which weakens the radiative cooling channel and makes the cooler temperature get a temporary rise. The cloudy sky condition can also be evidenced by the sudden rise of the atmospheric radiation curve present in Fig. 5b. To further investigate the relation between the temperature rise and atmospheric radiation rise, a dimensionless parameter is used to describe the variable of the cooler temperature and atmospheric radiation. It can be found in Fig. 6 that the change of temperature is nearly consistent with the vibration of the atmospheric radiation, indicating

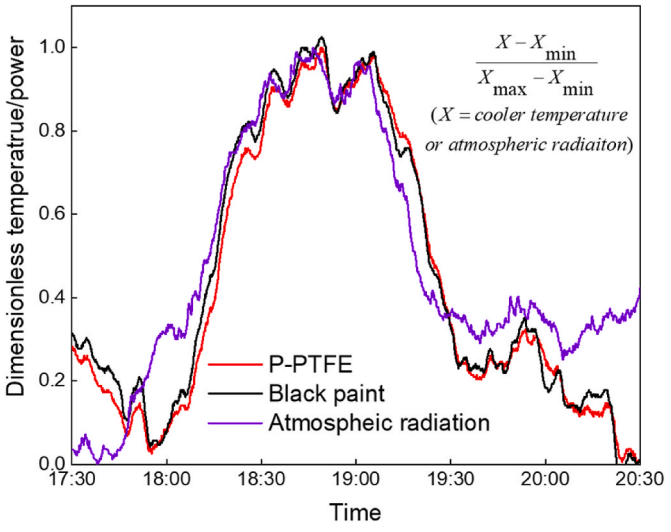

Fig. 6. Dimensionless cooler temperature and atmospheric radiation during nighttime testing.

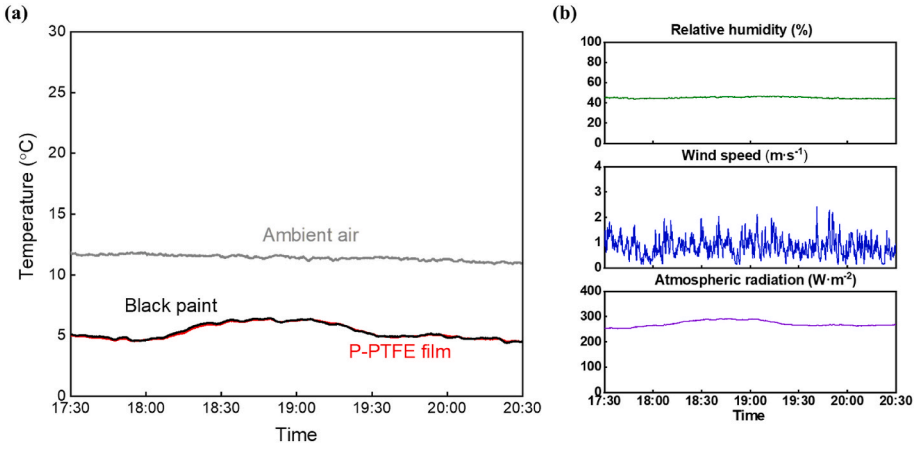

Fig. 5. (a) Measured temperature of the black paint cooler and P-PTFE during the nighttime, with ambient temperature plotted as a reference. (b) Measured relative humidity, wind speed, and long-wave atmospheric radiation.

that the increased atmospheric radiation due to the cloudy cover is the main reason for the temperature rise of the cooler in Fig. 5a.

3. Thermal analysis

3.1. Mathematical model

A theoretical model is developed to further investigate the radiative cooling performance under diffuse solar irradiance. As shown in Fig. 7, the radiative cooler absorbs diffuse solar irradiance and atmospheric radiation. Besides, the cooler radiates thermal radiation out of the cooler and has a convection heat process with ambient air. The steady-state assumption is applied during the thermal modeling.

The energy balance equation of the radiative cooler can be expressed as:

$$Q_{rad} - Q_{ds} - Q_{atm} - Q_{con} = 0 \tag{1}$$

Q_{rad} is thermal radiation power of the cooler and is presented by:

$$Q_{rad} = 2\pi \int_0^{\infty} \int_0^{\frac{\pi}{2}} I_{bb}(\lambda, T_c)\varepsilon_c(\lambda, \theta)\sin\theta \cos\theta d\theta d\lambda \tag{2}$$

where, $I_{bb}(\lambda, \theta)$ is the spectral radiance density of the blackbody at cooler temperature T_c, $\varepsilon_c(\lambda, \theta)$ is the spectral angular emissivity of the radiative cooler.

Q_{atm} is absorbed atmospheric radiation:

$$Q_{atm} = 2\pi \int_0^{\infty} \int_0^{\frac{\pi}{2}} I_{bb}(\lambda, T_a)\varepsilon_{atm}(\lambda, \theta)\alpha_c(\lambda, \theta)\sin\theta \cos\theta d\theta d\lambda \tag{3}$$

where T_a denotes ambient temperature, $\varepsilon_{atm}(\lambda, \theta)$ is the spectral angular emissivity of the atmosphere and can be obtained by a correlation related to the atmospheric transmittance at the vertical direction $\varepsilon_{atm}(\lambda, \theta)=1\text{-}\tau(\lambda, 0)^{1/\cos\theta}$, $\alpha_c(\lambda, \theta)$ is the spectral angular emissivity of the cooler.

Q_{con} is convection heat transfer power from ambient air to the radiative cooler, and Q_{ds} is absorbed diffuse solar irradiance:

$$Q_{con} = h(T_a - T_c) \tag{4}$$

$$Q_{ds} = \alpha_{eff} G_{ds} \tag{5}$$

where h denotes the overall heat transfer coefficient between the cooler and ambient air and can be estimated by a correlation that relates to wind speed $h = 2.5 + 2v$ [3], α_{eff} is AM 1.5 solar spectrum weighted solar absorptivity of the cooler, G_{ds} is diffuse solar irradiance. Notably, if the cooler is fixed with a tilt angle, the diffuse solar irradiance can be calculated by the Perez model [47] which considers the anisotropy property of the diffuse solar irradiance on the tilted surface. In the Perez model, the effects of the incidence angles of the cone of circumsolar irradiance on the tilted surface, the circumsolar and horizon brightness coefficients, tilted angle, and diffuse solar irradiance on the horizontal surface are comprehensively considered.

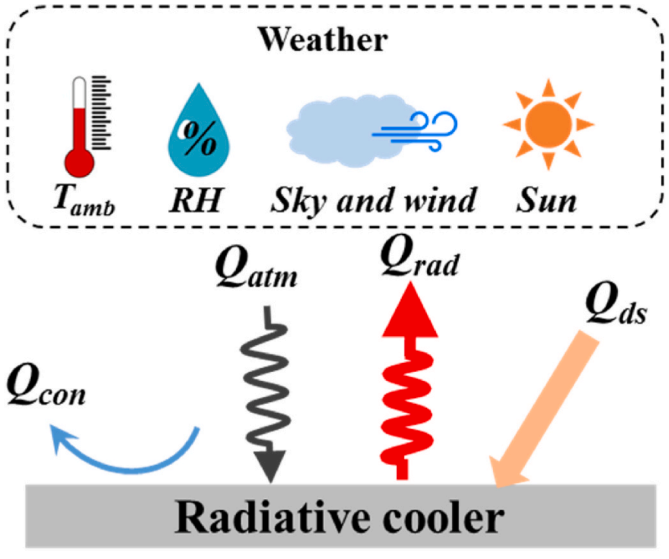

Fig. 7. Energy balance model of the radiative cooler under diffuse solar irradiance.

The equilibrium temperature of the cooler and the maximum cooling power of the cooler are two widely used indicators to evaluate the radiative cooling performance. The equilibrium temperature of the cooler is obtained from Equation (1) and the maximum cooling power is obtained when the cooler temperature is equal to ambient temperature. Here, the maximum temperature reduction of the cooler compared to ambient temperature and maximum cooling power is used to describe the cooling performance of the cooler.

3.2. The effect of environment parameters

The maximum temperature reduction and maximum cooling power of the black paint and P-PTFE are predicted under different solar irradiance. Ambient temperature of 300 K and overall heat transfer coefficient h of 6.9 $W{\cdot}m^{-2}{\cdot}K^{-1}$ [17] are used for calculation. Atmospheric transmittance of Mid-Latitude Winter is also used for calculation [48]. As shown in Fig. 8a, the maximum temperature reduction and maximum cooling power of the black paint reduce with increased solar irradiance. It can be found that the black paint (Fig. 8a) cannot be cooled to below ambient when the solar irradiance is larger than 100 W m^{-2} due to its ultra-high solar absorptivity. In contrast, the P-PTFE (Fig. 8b) can achieve sub-ambient radiative cooling because of its high solar reflection, even at solar irradiance of 1000 W m^{-2}. When solar irradiance is zero (i.e., at night), the maximum temperature drop and maximum cooling power of the black paint are 8.5°C and 95.3 W m^{-2}, while those for P-PTFE are 8.1°C and 90.1 W m^{-2}. Notably, with the proposed sunlight blocking strategy implementation, only diffuse solar irradiance affects the radiative cooling of the cooler and the level of diffuse sunlight is generally low.

The sky condition also affects the radiative cooling performance of the cooler. Four typical kinds of atmospheric transmittance profiles, including Mid-Latitude Winter (ML-W), Mid-Latitude Summer (ML-S), Tropical, and US standard 1976, are selected for comparison (Fig. 9a). During the calculation, diffuse solar irradiance is respectively set as 0, 100, 200, and 300 W m^{-2}. It can be seen that the sub-ambient cooling effect can be maintained for black paint (Fig. 9b) only under ML-W with solar irradiance of 0 and 100 W m^{-2}, which is consistent with the conclusion obtained from Fig. 8a, while the P-PTFE (Fig. 9c) can obtain sub-ambient cooling under all conditions. Importantly, the ML-W condition is friendliest for sub-ambient radiative cooling because the cooler can get the lowest temperature under ML-W, when compared with other sky conditions.

The effect of the non-radiative heat transfer process is also investigated based on different overall heat transfer coefficients (i.e., h) between the cooler and ambient air. During the calculation, h is set from 3 $W{\cdot}m^{-2}{\cdot}K^{-1}$ to 10 $W{\cdot}m^{-2}{\cdot}K^{-1}$, which corresponds to about 0.6 m s^{-1} to 3.8 m s^{-1}. As shown in Fig. 10, it can be seen that the temperature reduction of the black paint (Fig. 10a) and P-PTFE (Fig. 10b) decrease with increasing h when diffuse solar irradiance is 0, showing that radiative cooling performance is reduced due to the strong parasitic cooling loss. For P-PTFE, the temperature reduction reduces from 13.3°C to 6.6°C, when h changes from 3 $W{\cdot}m^{-2}{\cdot}K^{-1}$ to 10 $W{\cdot}m^{-2}{\cdot}K^{-1}$. When diffuse solar irradiance increase to 200 W m^{-2}, the black paint can't achieve sub-ambient cooling, and cooler temperature is higher than ambient temperature, so increasing h can enhance the heat dissipation of the black paint and reduce the temperature difference between the black paint and ambient air. Under diffuse solar irradiance of 200 W m^{-2}, the P-PTFE can still achieve sub-ambient cooling, but performance will

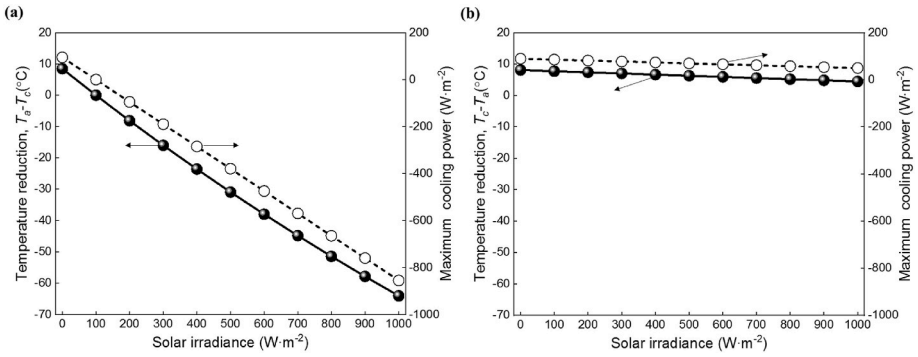

Fig. 8. Maximum temperature reduction and maximum cooling power of the (a) black paint, and (b) P-PTFE, under different solar irradiance.

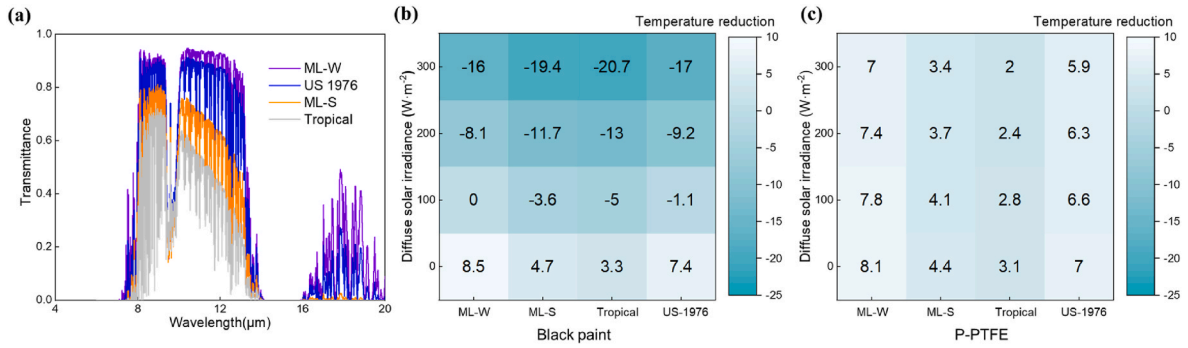

Fig. 9. (a) Transmittance of the atmosphere under different profiles. (b) Maximum temperature reduction of the black paint. (c) Maximum temperature reduction of the PTFE.

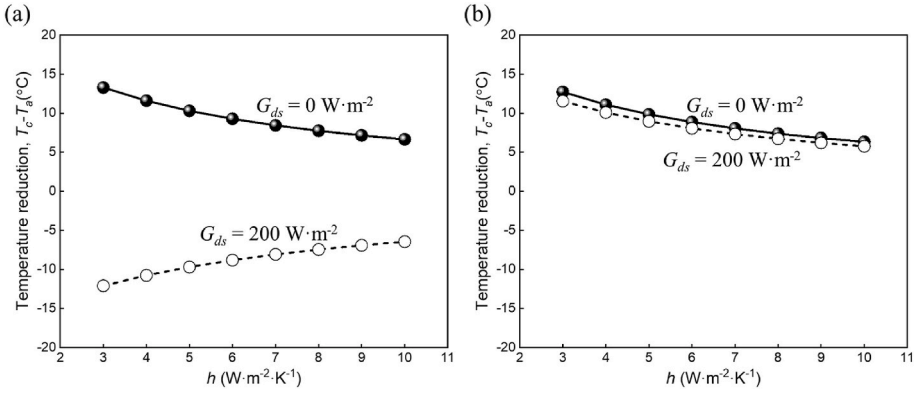

Fig. 10. Maximum temperature reduction of the (a) black paint, and (b) P-PTFE, under different *h*.

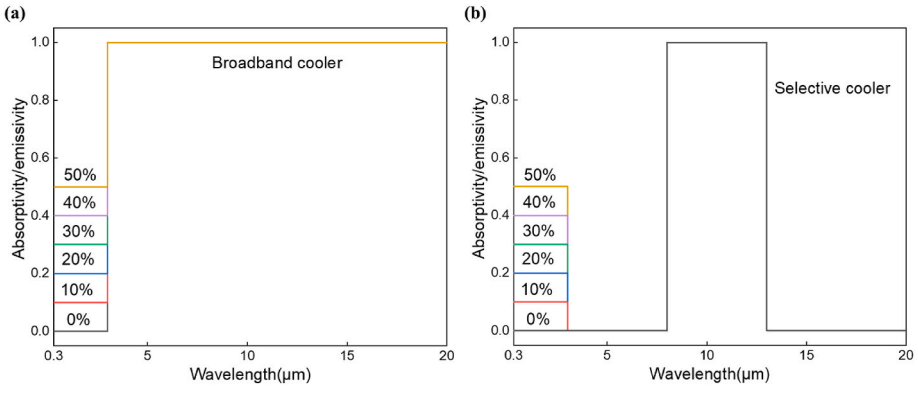

Fig. 11. (a) Emissivity of broadband cooler, and (b) selective cooler, with different solar absorption.

degenerate with high values of h.

3.3. The effect of cooler spectrum

The cooler spectrum is the key to sub-ambient radiative cooling. Selective spectrum and broadband spectrum are widely recognized as two kinds of ideal spectrum for efficient radiative cooling. In this subsection, different spectrums that include selective infrared emission and broadband infrared emission with different solar absorptivity are analyzed and compared. The spectrums of cooler are shown in Fig. 11, which shows broadband cooler and selective cooler with solar absorption of 0%, 10%, 20%, 30%, 40%, and 50%. The maximum temperature reduction of the cooler with the above spectrums is predicted under the ambient temperature of 300 K, an overall heat transfer coefficient of 6.9 $W{\cdot}m^{-2}{\cdot}K^{-1}$, and diffuse solar irradiance of 200 W m^{-2}.

It is found from Fig. 12(a) that the temperature reduction of the cooler will reduce with the increased solar absorption regardless of broadband and selective emission. Besides, the selective cooler is more sensitive to the solar absorption because the temperature reduction of the selective cooler is higher than that of the broadband cooler when solar absorption is lower than 30%, while this condition reverses when solar absorption is 40%. For instance, the temperature reduction of the selective cooler is 11.2°C under solar absorption of 0%, which is 1.8°C higher than that of the broadband cooler. When solar absorption increases to 50%, the temperature reduction of the selective cooler is 0.2°C, which is 0.8°C lower than that of the broadband cooler. This result indicates that the proposed sunlight blocking strategy may be more useful for selective coolers. Notably, the difference between the broadband cooler and selective cooler in Fig. 12a is not remarkable and this may be due to the larger parasitic cooling loss power. In Fig. 12b where the overall heat transfer coefficient is suppressed, the difference is obviously enlarged, which shows selective cooler with small solar absorption can get a lower stagnation temperature than the broadband cooler because of the selective emission property. Moreover, it can also be evidenced by Fig. 12b that the selective cooler is more sensitive to solar absorption.

3.4. Cooling performance comparison

In this subsection, a broadband cooler with 20% solar absorption is selected to evaluate the maximum radiative cooling power with and without the proposed sunlight blocking strategy. Hourly climatic data of Lhasa, China obtained from the website of the software EnergyPlus [49] is used for the simulation and is shown in Fig. 13a. It can be found that diffuse solar irradiance is small for clear sunny days and will increase on partly cloudy days. As shown in Fig. 13b, the maximum cooling power of the broadband cooler with 20% solar absorption is negative during the daytime, which indicates the cooler can't achieve sub-ambient radiative cooling under sunlight. This is because 20% solar absorption will attribute a solar heating power of over 100 W m^{-2} and completely counteract the cooling effect generated by long-wave thermal radiation. When the sunlight blocking strategy is applied, the effect of direct sunlight is eliminated and then the maximum cooling power of the cooler becomes positive, showing that the sub-ambient cooling phenomenon is successfully obtained, even the cooler has 20% solar absorption. For instance, the maximum cooling power of the cooler with the sunlight blocking strategy is 66 W m^{-2} when total solar irradiance and ambient temperature are 788 W m^{-2} and 1.5°C, while the cooler without the sunlight blocking strategy is heated above ambient temperature with a solar heating power of 84 W m^{-2}, proving the feasibility of the proposed strategy for daytime sub-ambient radiative cooling. Notably, if the diffuse solar irradiance dominates the solar radiation due

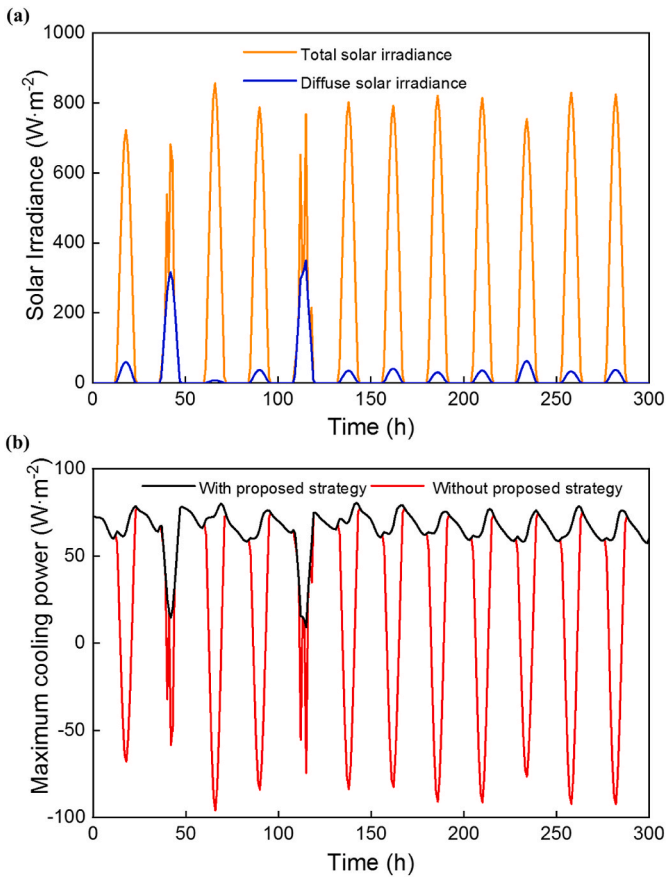

Fig. 13. (a) Hourly total solar irradiance and diffuse solar irradiance in Lhasa, China. (b) Maximum cooling power of the broadband cooler with 20% solar absorption with and without proposed sunlight blocking strategy.

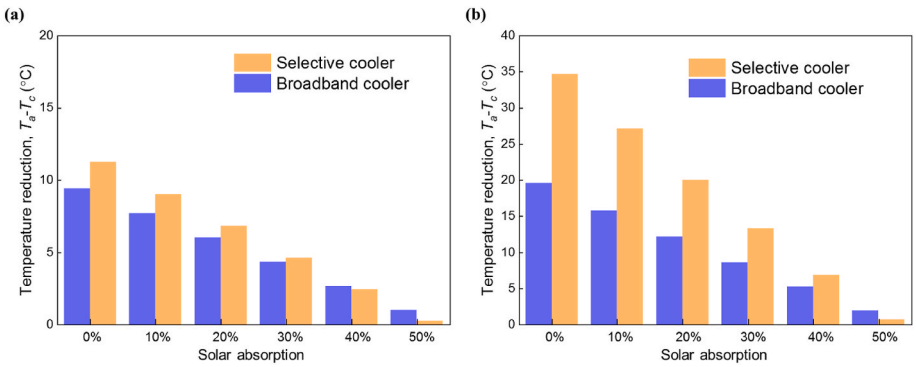

Fig. 12. Maximum temperature reduction of the broadband and selective cooler with different solar absorption under overall heat transfer coefficient h of (a) 6.9 $W{\cdot}m^{-2}{\cdot}K^{-1}$, and (b) 1.0 $W{\cdot}m^{-2}{\cdot}K^{-1}$.

to the bad weather condition, the assistant methods, including using an infrared-reflective mirror cone or solar reflective windshields, can be coupled with the proposed strategy and still used for sub-ambient radiative cooling.

4. Conclusions

A feasible sunlight blocking strategy based on geometrical optics is proposed for radiative coolers to reduce the effect of direct solar radiation on sub-ambient radiative cooling. A ring-like shield is implemented to passively decouple the radiative cooler from the direct solar radiation that is the domination of the solar irradiance by preventing the propagation of direct sunlight. Two radiative coolers, including a black paint cooler (solar absorptive cooler) and P-PTFE (solar reflective cooler), are fabricated and spectrally tested for outdoor experimental demonstration. Experiment results show that the black paint cooler and P-PTFE can be cooled to 3.5°C and 6.5°C below ambient temperature under average solar radiation of 500 W m^{-2}, revealing that the proposed sunlight blocking strategy contributes to sub-ambient radiative cooling, especially for common materials with non-negligible solar absorption. Theoretical analysis also proves the effectiveness of the sunlight blocking strategy and reveals that radiative cooler with selective emission in the atmospheric window is more sensitive to sunlight, indicating that selective cooler can remarkably benefit from the sunlight blocking strategy. In summary, an easy method is demonstrated to be effective to improve the sub-ambient radiative cooling performance and promises to be used as a practical implementation.

Data availability

The data that support the findings of this study are available from the corresponding author upon reasonable request.

CRediT authorship contribution statement

Bin Zhao: Writing – review & editing, Writing – original draft, Project administration, Methodology, Investigation, Funding acquisition, Conceptualization. **Kegui Lu:** Writing – review & editing, Investigation, Formal analysis, Data curation. **Mingke Hu:** Writing – review & editing, Resources, Funding acquisition, Formal analysis. **Ke Wang:** Writing – review & editing, Methodology, Formal analysis. **Datong Gao:** Writing – review & editing, Software, Formal analysis. **Ken Chen:** Writing – review & editing, Resources, Formal analysis. **Qingdong Xuan:** Writing – review & editing, Methodology, Formal analysis. **Gang Pei:** Writing – review & editing, Supervision, Project administration, Funding acquisition, Formal analysis, Conceptualization.

Declaration of competing interest

The authors declare that they have no known competing financial interests or personal relationships that could have appeared to influence the work reported in this paper.

Acknowledgments

This work was supported by the National Natural Science Foundation of China (NSFC 52106276, 52130601, and 51906241), Project funded by China Postdoctoral Science Foundation (2020TQ0307 and 2020M682033), and Fundamental Research Funds for the Central Universities (WK2090000028).

References

[1] B. Zhao, M. Hu, X. Ao, N. Chen, G. Pei, Radiative cooling: a review of fundamentals, materials, applications, and prospects, Appl. Energy 236 (2019) 489–513, https://doi.org/10.1016/j.apenergy.2018.12.018.

[2] B. Zhao, M. Hu, X. Ao, Q. Xuan, G. Pei, Spectrally selective approaches for passive cooling of solar cells: a review, Appl. Energy 262 (2020), 114548, https://doi.org/10.1016/j.apenergy.2020.114548.

[3] D. Zhao, A. Aili, Y. Zhai, S. Xu, G. Tan, X. Yin, R. Yang, Radiative sky cooling: Fundamental principles, materials, and applications, Appl. Phys. Rev. 6 (2019), 021306, https://doi.org/10.1063/1.5087281.

[4] S. Fan, A. Raman, Metamaterials for radiative sky cooling, Natl. Sci. Rev. 5 (2018) 132–133, https://doi.org/10.1093/nsr/nwy012.

[5] X. Yin, R. Yang, G. Tan, S. Fan, Terrestrial radiative cooling: using the cold universe as a renewable and sustainable energy source, Science 370 (2020) 786–791, https://doi.org/10.1126/science.abb0971, 80-.

[6] S. Fan, W. Li, Photonics and thermodynamics concepts in radiative cooling, Nat. Photonics (2022), https://doi.org/10.1038/s41566-021-00921-9.

[7] O.F. Curtis, Leaf temperatures and the cooling of leaves by radiation, Plant Physiol. 11 (1936) 343.

[8] W.C. Swinbank, Longwave radiation from clear sky, Q. J. R. Meteorol. Soc. 89 (1963) 339–348.

[9] B. Bartoli, S. Catalanotti, B. Coluzzi, V. Cuomo, V. Silvestrini, G. Troise, Nocturnal and diurnal performances of selective radiators, Appl. Energy 3 (1977) 267–286, https://doi.org/10.1016/0306-2619(77)90015-0.

[10] D. Michell, K.L. Biggs, Radiation cooling of buildings at night, Appl. Energy 5 (1979) 263–275, https://doi.org/10.1016/0306-2619(79)90017-5.

[11] B. Bartoli, B. Coluzzi, V. Silvestrini, A. Addeo, L. Nicolais, G. Romero, Light selective structures for large scale natural air conditioning, Sol. Energy 24 (1980) 93–98, https://doi.org/10.1016/0038-092X(80)90024-9.

[12] B. Zhao, M. Hu, X. Ao, Q. Xuan, Z. Song, G. Pei, Is it possible for a photovoltaic-thermoelectric device to generate electricity at night? Sol. Energy Mater. Sol. Cells 228 (2021), 111136 https://doi.org/10.1016/j.solmat.2021.111136.

[13] A.P. Raman, W. Li, S. Fan, Generating light from darkness, Joule 3 (2019) 2679–2686, https://doi.org/10.1016/j.joule.2019.08.009.

[14] B. Zhao, G. Pei, A.P. Raman, Modeling and optimization of radiative cooling based thermoelectric generators, Appl. Phys. Lett. 117 (2020), 163903, https://doi.org/10.1063/5.0022667.

[15] C. Lin, Y. Li, C. Chi, Y.S. Kwon, J. Huang, Z. Wu, J. Zheng, G. Liu, C.Y. Tso, C.Y. H. Chao, B. Huang, A solution-processed inorganic emitter with high spectral selectivity for efficient subambient radiative cooling in hot humid climates, Adv. Mater. (2022), 2109350, https://doi.org/10.1002/adma.202109350, 2109350.

[16] X. Ao, B. Li, B. Zhao, M. Hu, H. Ren, H. Yang, J. Liu, J. Cao, J. Feng, Y. Yang, Z. Qi, L. Li, C. Zou, G. Pei, Self-adaptive integration of photothermal and radiative cooling for continuous energy harvesting from the sun and outer space, Proc. Natl. Acad. Sci. USA 119 (2022) 1–7, https://doi.org/10.1073/pnas.2120557119.

[17] A.P. Raman, M.A. Anoma, L. Zhu, E. Rephaeli, S. Fan, Passive radiative cooling below ambient air temperature under direct sunlight, Nature 515 (2014) 540–544, https://doi.org/10.1038/nature13883.

[18] Y. Zhai, Y. Ma, S.N. David, D. Zhao, R. Lou, G. Tan, R. Yang, X. Yin, Scalable-manufactured randomized glass-polymer hybrid metamaterial for daytime radiative cooling, Science 355 (2017) 1062–1066, https://doi.org/10.1126/science.aai7899, 80-.

[19] J. Mandal, Y. Fu, A.C. Overvig, M. Jia, K. Sun, N.N. Shi, H. Zhou, X. Xiao, N. Yu, Y. Yang, Hierarchically porous polymer coatings for highly efficient passive daytime radiative cooling, Science 362 (2018) 315–319, https://doi.org/10.1126/science.aat9513, 80-.

[20] E. Rephaeli, A. Raman, S. Fan, Ultrabroadband photonic structures to achieve high-performance daytime radiative cooling, Nano Lett. 13 (2013) 1457–1461, https://doi.org/10.1021/nl4004283.

[21] W. Li, Y. Shi, Z. Chen, S. Fan, Photonic thermal management of coloured objects, Nat. Commun. 9 (2018) 4240, https://doi.org/10.1038/s41467-018-06535-0.

[22] L. Zhu, A.P. Raman, S. Fan, Radiative cooling of solar absorbers using a visibly transparent photonic crystal thermal blackbody, Proc. Natl. Acad. Sci. USA 112 (2015) 12282–12287, https://doi.org/10.1073/pnas.1509453112.

[23] B. Zhao, K. Lu, M. Hu, J. Liu, L. Wu, C. Xu, Q. Xuan, G. Pei, Radiative cooling of solar cells with micro-grating photonic cooler, Renew. Energy 191 (2022) 662–668, https://doi.org/10.1016/j.renene.2022.04.063.

[24] H. Zhong, Y. Li, P. Zhang, S. Gao, B. Liu, Y. Wang, T. Meng, Y. Zhou, H. Hou, C. Xue, Y. Zhao, Z. Wang, Hierarchically hollow microfibers as a scalable and effective thermal insulating cooler for buildings, ACS Nano (2021), https://doi.org/10.1021/acsnano.1c01814.

[25] K. Zhou, W. Li, B.B. Patel, R. Tao, Y. Chang, S. Fan, Y. Diao, L. Cai, Three-dimensional printable nanoporous polymer matrix composites for daytime radiative cooling, Nano Lett. 21 (2021) 1493–1499, https://doi.org/10.1021/acs.nanolett.0c04810.

[26] Y. Chen, B. Dang, J. Fu, C. Wang, C. Li, Q. Sun, H. Li, Cellulose-based hybrid structural material for radiative cooling, Nano Lett. 21 (2021) 397–404, https://doi.org/10.1021/acs.nanolett.0c03738.

[27] M. Chen, S. Li, D. Pang, Y. Zhao, Y. Yang, H. Yan, Numerically enhancing daytime radiative cooling performance of random dielectric microsphere coatings by hollow structures, J. Photon. Energy 11 (2021) 1–13, https://doi.org/10.1117/1.JPE.11.042108.

[28] Z. Cheng, H. Han, F. Wang, Y. Yan, X. Shi, H. Liang, X. Zhang, Y. Shuai, Efficient radiative cooling coating with biomimetic human skin wrinkle structure, Nano Energy 89 (2021), 106377, https://doi.org/10.1016/j.nanoen.2021.106377.

[29] J. Mandal, Y. Yang, N. Yu, A.P. Raman, Paints as a scalable and effective radiative cooling Technology for buildings, Joule 4 (2020) 1350–1356, https://doi.org/10.1016/j.joule.2020.04.010.

[30] X. Li, J. Peoples, P. Yao, X. Ruan, Ultrawhite BaSO4 paints and films for remarkable daytime subambient radiative cooling, ACS Appl. Mater. Interfaces 13 (2021) 21733–21739, https://doi.org/10.1021/acsami.1c02368.
[31] X. Ao, M. Hu, B. Zhao, N. Chen, G. Pei, C. Zou, Preliminary experimental study of a specular and a diffuse surface for daytime radiative cooling, Sol. Energy Mater. Sol. Cells 191 (2019) 290–296, https://doi.org/10.1016/j.solmat.2018.11.032.
[32] H. Bao, C. Yan, B. Wang, X. Fang, C.Y. Zhao, X. Ruan, Double-layer nanoparticle-based coatings for efficient terrestrial radiative cooling, Sol. Energy Mater. Sol. Cells 168 (2017) 78–84, https://doi.org/10.1016/j.solmat.2017.04.020.
[33] J. Huang, M. Li, D. Fan, Core-shell particles for devising high-performance full-day radiative cooling paint, Appl. Mater. Today 25 (2021), 101209, https://doi.org/10.1016/j.apmt.2021.101209.
[34] E. Torgerson, J. Hellhake, Polymer solar filter for enabling direct daytime radiative cooling, Sol. Energy Mater. Sol. Cells 206 (2020), 110319, https://doi.org/10.1016/j.solmat.2019.110319.
[35] J. Zhang, Z. Zhou, J. Quan, D. Zhang, J. Sui, J. Yu, J. Liu, A flexible film to block solar radiation for daytime radiative cooling, Sol. Energy Mater. Sol. Cells 225 (2021), 111029, https://doi.org/10.1016/j.solmat.2021.111029.
[36] J. Zhang, Z. Zhou, H. Tang, J. Xing, J. Quan, J. Liu, J. Yu, M. Hu, Mechanically robust and spectrally selective convection shield for daytime subambient radiative cooling, ACS Appl. Mater. Interfaces (2021), 0c21204, https://doi.org/10.1021/acsami.0c21204 acsami.
[37] A. Leroy, B. Bhatia, C.C. Kelsall, A. Castillejo-Cuberos, M. Di Capua H, L. Zhao, L. Zhang, A.M. Guzman, E.N. Wang, High-performance subambient radiative cooling enabled by optically selective and thermally insulating polyethylene aerogel, Sci. Adv. 5 (2019), eaat9480, https://doi.org/10.1126/sciadv.aat9480.
[38] J.J. García-Esteban, J. Bravo-Abad, J.C. Cuevas, Deep learning for the modeling and inverse design of radiative heat transfer, Phys. Rev. Appl. 16 (2021), 064006, https://doi.org/10.1103/PhysRevApplied.16.064006.
[39] J. Song, J. Seo, J. Han, J. Lee, B.J. Lee, Ultrahigh emissivity of grating-patterned PDMS film from 8 to 13 μ m wavelength regime, Appl. Phys. Lett. 117 (2020), 094101, https://doi.org/10.1063/5.0017838.
[40] Z. Chen, L. Zhu, A. Raman, S. Fan, Radiative cooling to deep sub-freezing temperatures through a 24-h day–night cycle, Nat. Commun. 7 (2016), 13729, https://doi.org/10.1038/ncomms13729.
[41] B. Zhao, X. Ao, N. Chen, Q. Xuan, M. Hu, G. Pei, General strategy of passive sub-ambient daytime radiative cooling, Sol. Energy Mater. Sol. Cells 199 (2019) 108–113, https://doi.org/10.1016/j.solmat.2019.04.028.
[42] D. Zhao, A. Aili, Y. Zhai, J. Lu, D. Kidd, G. Tan, X. Yin, R. Yang, Subambient cooling of water: toward real-world applications of daytime radiative cooling, Joule 3 (2019) 111–123, https://doi.org/10.1016/j.joule.2018.10.006.
[43] A. Aili, D. Zhao, J. Lu, Y. Zhai, X. Yin, G. Tan, R. Yang, A kW-scale, 24-hour continuously operational, radiative sky cooling system: experimental demonstration and predictive modeling, Energy Convers. Manag. 186 (2019) 586–596, https://doi.org/10.1016/j.enconman.2019.03.006.
[44] J. Liu, D. Zhang, S. Jiao, Z. Zhou, Z. Zhang, F. Gao, Preliminary study of radiative cooling in cooling season of the humid coastal area, Sol. Energy Mater. Sol. Cells 208 (2020), 110412, https://doi.org/10.1016/j.solmat.2020.110412.
[45] B. Bhatia, A. Leroy, Y. Shen, L. Zhao, M. Gianello, D. Li, T. Gu, J. Hu, M. Soljačić, E. N. Wang, Passive directional sub-ambient daytime radiative cooling, Nat. Commun. 9 (2018) 5001, https://doi.org/10.1038/s41467-018-07293-9.
[46] H. Zhong, P. Zhang, Y. Li, X. Yang, Y. Zhao, Z. Wang, Highly solar-reflective structures for daytime radiative cooling under high humidity, ACS Appl. Mater. Interfaces 12 (2020) 51409–51417, https://doi.org/10.1021/acsami.0c14075.
[47] R. Perez, P. Ineichen, R. Seals, J. Michalsky, R. Stewart, Modeling daylight availability and irradiance components from direct and global irradiance, Sol. Energy 44 (1990) 271–289, https://doi.org/10.1016/0038-092X(90)90055-H.
[48] MODTRAN Infrared Light in the Atmosphere. http://climatemodels.uchicago.edu/modtran/.
[49] Weather data. https://energyplus.net/weather.